ACS OMEGA

http://pubs.acs.org/journal/acsodf

Article

A Lysosome-Targeted Near-Infrared Fluorescent Probe with Excellent Water Solubility for Surgery Navigation in Breast Cancer

Yumei Wu, Zhengjun Chen, Dan Shen, Zhiquan He, Jiajia Lv, Hongyu Li, Mingyan Yang, Jun Tan, Jianrong Yuan, Jie Gao,* and Zeli Yuan*

Cite This: *ACS Omega* 2023, 8, 12481−12488

Read Online

ACCESS | Metrics & More | Article Recommendations | Supporting Information

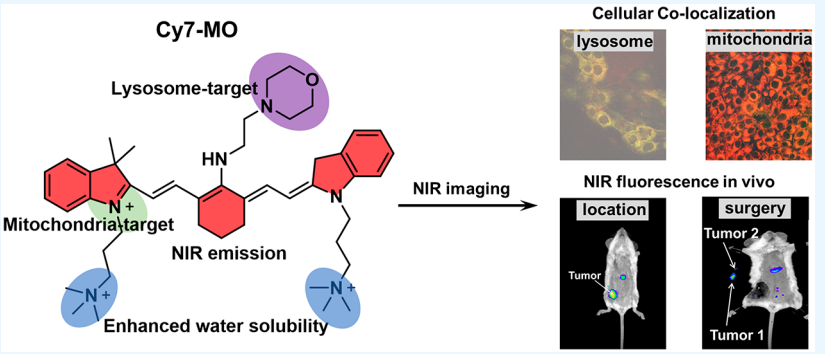

ABSTRACT: To get a tumor-targeted contrast agent for imaging guide resection of tumors, we designed a novel fluorescent probe based on the heptamethine cyanine core, Cy7-MO, which has excellent water solubility and near-infrared photophysical and lysosomal targeting properties. The chemical structure of Cy7-MO was characterized by nuclear magnetic resonance spectroscopy and high-resolution mass spectrometry. The toxicity of Cy7-MO was evaluated by cell counting kit-8. Then, a cellular-level study was conducted to evaluate the suborganelle localization in 4T1-Luc1 cells, and it was also used for surgical navigation in orthotopic breast tumor resection *in vivo*. The results showed that Cy7-MO was well targeted to lysosomes. Importantly, the Cy7-MO probe was found to be well tolerable and exhibited excellent biocompatibility. Moreover, the orthotopic breast tumor margin was clearly visualized through fluorescence guiding of Cy7-MO. Finally, the correct tumor tissues were completely removed, and a negative margin was obtained successfully, which demonstrated an enhanced precision of surgery.

INTRODUCTION

According to the latest report from the International Agency for Research on Cancer, there were more than 2.26 million new cases of breast cancer worldwide in 2020, accounting for about 11.7% of all newly diagnosed cancers. Breast cancer is the most common malignant tumor in the world, and is also the leading cause of cancer death among women.[1−3] The primary treatment for most breast cancers is surgery, and the complete removal of tumor tissue is essential to prolong a patient's life or even cure the cancer completely.[4−6] However, inadequate detection of breast tumor margins has been shown to be associated with poor prognosis. Traditional surgery involves either incomplete removal of the tumor or unnecessary removal of healthy tissue. If the tumor is incomplete, additional tissue excision should be performed. However, this intraoperative evaluation is time-consuming and dependent on the experience of the surgeon. In fact, some studies have shown that about 20−50% of breast cancer patients have positive tumor margins after lumpectomy.[7] The presence of multiple positive margins is a risk factor for cancer recurrence and poor survival, and different surgical margins could have different prognostic roles.[8] So, before surgery, basic information such as the size, number, and location of the tumors inside the body has to be confirmed, which requires the imaging technique to have excellent spatial resolution and high sensitivity.[9,10] Other conventional imaging techniques, such as computed tomography and magnetic resonance imaging, are generally difficult to integrate into the operating room.[11] Most importantly, these conventional imaging modalities cannot reliably communicate real-time feedback to the surgeon and have limited tumor specificity.[12] Thus, it is imperative to develop intraoperative imaging techniques to accurately delineate the tumor margin, and the imaging technique with superb sensitivity and prominent signal-to-background ratio is highly desirable intraoperatively.[13]

Received: January 30, 2023
Accepted: March 13, 2023
Published: March 23, 2023

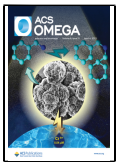

To address this pressing clinical challenge, fluorescence image-guided surgery has emerged as a promising strategy for using fluorescence to highlight tumor tissue. As a kind of noninvasive molecular imaging technology, near-infrared (NIR) fluorescence imaging is characterized by high sensitivity in deep tissue, high spatial resolution and safety, and easy to use.[14−17] In recent years, it has received more and more attention in preoperative diagnosis and intraoperative guidance. However, existing fluorescence imaging methods still have some limitations. For example, indocyanine green (ICG) is a fluorescent dye approved by the Food and Drug Administration for visualization of human tumors,[18] but has been limited to slow blood clearance and lack of specificity.[19,20]

Therefore, it is urgent to develop targeted and safe contrast agents to guide the resection of cancer tumors. Currently, the use of cyanine dyes for cancer imaging and treatment has received increasing attention.[21−23] Cyanine 7 (Cy7) is a NIR anthocyanin fluorescent dye,[24,25] which has weak background fluorescence and strong penetration characteristics, so Cy7 is often used *in vivo* imaging of small animals,[26] but the water solubility of ordinary Cy7 is low. In view of the poor water solubility of conventional cyanine dyes, quaternary ammonium groups were modified on each side to provide good water solubility according to a previous report.[27] Compared with normal cells, cancer cells contain more lysosomes that can be employed as targets for fluoresce imaging probe.[28] In our previous work,[29] a morpholine moiety was introduced on the IR780 (a heptamethine cyanine derivative) to improve the tumor-targeted potency.

In the present work, to enable the application of fluorescent surgical navigation for the precise resection of tumors *in vivo*, we designed a fluorescent probe Cy7-MO (Scheme 1) with excellent NIR photophysical properties and lysosomal targeting based on the heptamethine cyanine core. Then, the chemical structure of Cy7-MO was characterized by nuclear magnetic resonance (NMR) spectroscopy and high-resolution mass spectrometry (HRMS). It was performed at the cellular level to study the toxicity and suborganelle localization of 4T1-Luc1 cells. It was also used for surgical navigation in orthotopic breast tumor resection *in vivo*. The results showed that Cy7-MO was well targeted to tumor lysosomes and effectively delineated tumor margins to guide tumor resection.

Scheme 1. Synthetic Procedure of Cy7-MO

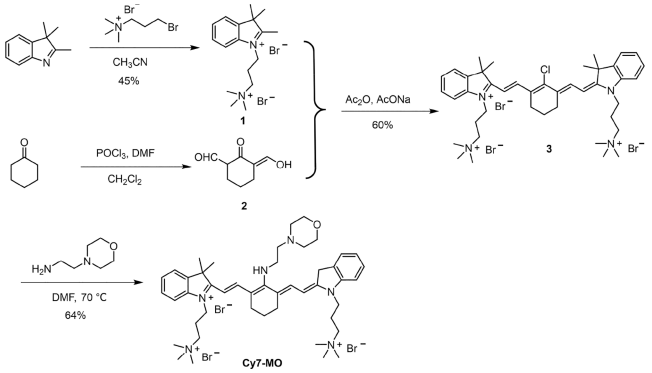

RESULTS AND DISCUSSION

2.1. Synthesis, Characterization, and Photophysical Properties of Cy7-MO. *2.1.1. Design, Synthesis, and Characterization of Cy7-MO.* To enable the application of fluorescent surgical navigation for the precise resection of tumors *in vivo*, we designed a fluorescent probe Cy7-MO based on the heptamethine cyanine core, due to its excellent NIR photophysical properties and mitochondrial targeting (Scheme 1). Because of the poor water solubility of conventional cyanine dyes, quaternary ammonium groups were modified on each side to provide good water solubility (60% yield) according to a previous report.[27] To permit subsequent lysosomal targeting, a morpholine moiety was introduced on the meso-chlorine atom to obtain the final probe Cy7-MO (64% yield). The chemical structure of Cy7-MO was characterized by NMR spectroscopy and HRMS (Figures S1−S3).

2.1.2. Photophysical Properties of Cy7-MO. Given that Cy7-MO possessed multiple positive charges, it exhibited good solubility in aqueous solutions, which facilitated subsequent biological applications. Therefore, the spectral properties of Cy7-MO were evaluated in PBS buffer (10 mM, pH 7.4) (Figure 1). Accordingly, Cy7-MO showed the maximum absorption at 637 nm. And in the fluorescence spectrum, the maximum emission wavelength of Cy7-MO was 759 nm. The Stokes shift value of Cy7-MO was 122 nm, which facilitates better bioimaging. The fluorescence quantum yield was measured as 2.7% using methylene blue as a standard (2% in water). In addition, the NIR fluorescence emission property of Cy7-MO was available for subsequent *in vivo* imaging and surgical navigation.

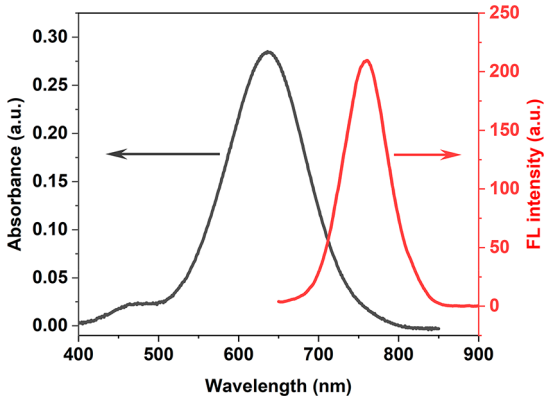

Figure 1. Absorbance (black line) and fluorescence (red line) spectra of Cy7-MO (10 μM) in PBS buffer (pH 7.4, 10 mM).

2.2. *In Vitro* Colocalization. *2.2.1. Cytotoxicity.* Cytotoxicity assays were carried out against 4T1-Luc1 breast cancer cell lines. The cells were incubated with different concentrations of Cy7-MO solution, and cell viability was measured using the cell counting kit-8 (CCK-8) assay. As can be seen from Figure S4, the concentration of Cy7-MO from 0 to 300 μM did not induce cytotoxic effects, with 90%∼120% viability at all evaluated concentrations which were all higher than 80%.

2.2.2. Cellular Colocalization. According to the literature, the acidity of the lysosome is much higher (pH 4.5−5.0) than that of other organelles,[30] and cancer cells possess more lysosomes in comparison to normal cells.[28] However, morpholine has low ionic strength and tends to target acidic subcellular organelles (such as lysosomes).[30] So, the dye molecules can achieve lysosome targeting by structurally modifying the morpholine structure.[31,32]

https://doi.org/10.1021/acsomega.3c00601
ACS Omega 2023, 8, 12481−12488

To identify the subcellular location of the Cy7-MO probe, the colocalization experiments were performed, and Lyso-Tracker Green and rhodamine 123 were used. As shown in Figure 2A, the fluorescence signals from Cy7-MO (red)

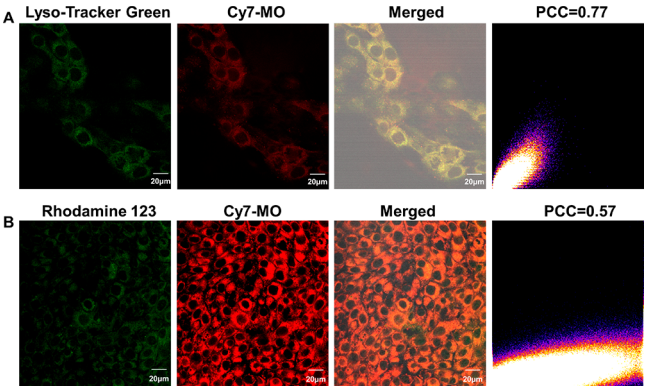

Figure 2. Colocalization studies of Cy7-MO in lysosome (A) and mitochondria (B) in 4T1-Luc1 cells (scale bar = 20 μm).

overlaid very well with those from Lyso-Tracker Green (Pearson's correlation coefficient (PCC) of 0.77). PCC between the fluorescence signal from Cy7-MO (red) in Figure 2B and that from rhodamine 123 was slightly lower (0.57). These two results indicated the strong affinity of morpholine group to lysosomes in Cy7-MO, while Cy7-MO had a slightly poorer affinity for mitochondria. The results of cell colocalization *in vitro* laid a certain experimental basis for the Cy7-MO probe targeting tumor tissue *in vivo*, which was expected to further achieve accurate tumor localization and navigational resection.

2.3. Safety Evaluation of Cy7-MO. The possible toxicity due to Cy7-MO was assessed by treating the mice with blank PBS and Cy7-MO solution. Accordingly, no mortality was observed during these studies, and no abnormal clinical signs or behaviors were observed in all groups of mice.

Then, the biochemical indices including aspartate aminotransferase (AST), glutamate transferase (ALT), creatinine (CREA), and urea (UREA) were measured to assess liver and kidney function. The reference ranges of these biochemical parameters in normal healthy BALB/c female mice were: ALT (43.79 ± 18.99 U/L), AST (146.4 ± 57.6 U/L), CREA (18.13 ± 6.76 μmol/L), UREA (8.13 ± 1.33 mmol/L).[33] The serum biochemical data are presented in Supporting Information (Figure S5), which showed Cy7-MO had no significant effect on liver and kidney function. In addition, the result of hematoxylin-eosin (H&E) staining showed that no noticeable histopathological changes or lesions were detected in main organs of all groups (Figure S6), suggesting that Cy7-MO was well tolerable and had excellent biocompatibility.

2.4. Cy7-MO-Guided Surgical Resection. *2.4.1. Biodistribution of Cy7-MO in Mice.* To determine the feasibility of tumor targeting and the optimal targeting time for precise surgery, mice were administered the Cy7-MO probe after being intravenously injected for real-time imaging of the probe. As shown in Figure 3A, the fluorescent signal was observed at about 5 min postinjection, but the signals in the bladder were strong and could not be separated from those in the tumor tissue. About 24 h later, the signal at the breast tumor area could be seen obviously. Figure 3B shows that with the extension of time, the fluorescence intensity of Cy7-MO

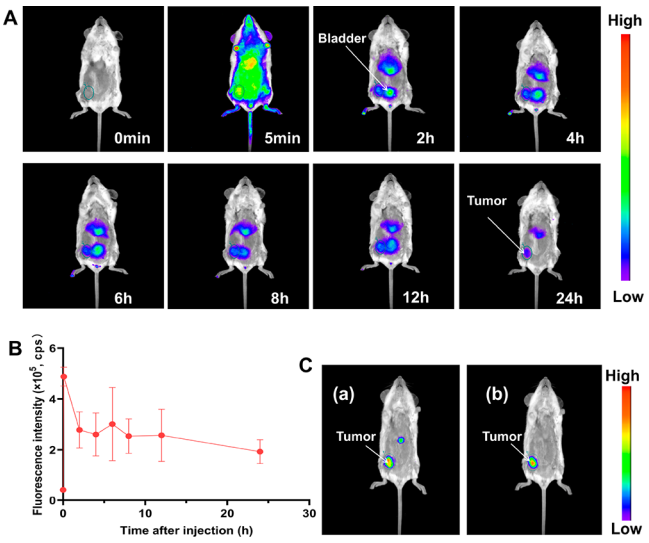

Figure 3. Fluorescence signal distribution and tumor location of Cy7-MO probe. (A) Fluorescence signal distribution of the Cy7-MO probe *in vivo* at different time points after intravenous injection of the probe using the Berthold equipment. (B) Fluorescence intensity of the tumor site as a function of postinjection time. Data are presented as the means ± SD (n = 3 mice). (C) Localization comparison of Cy7-MO fluorescence (a) and bioluminescence (b).

decreased gradually. Within 2 to 12 h after the injection of Cy7-MO, obvious fluorescence signals could be seen in the bladder (Figure 3A), indicating that the probe could be quickly excreted through the kidney after entering the body, thus reducing the toxic side effects and damage. These results indicated that the probe could be used to specifically visualize the microenvironment of orthotopic breast tumors and exhibited prolonged retention at the tumor area to guide surgery. Cy7-MO probe achieved low background and high signal-to-background ratio, which increased precision navigational surgical excision of a tumor.

2.4.2. Validation of Tumor Location. To verify the accuracy of Cy7-MO probe in tumor localization, the bioluminescence imaging and fluorescence imaging were performed successively in the same animals (n = 3). As can be seen from Figure 3C, the region located by Cy7-MO fluorescence (a) was basically consistent with that of bioluminescence (b), indicating that Cy7-MO probe was successfully and accurately located in breast cancer tissue and could be used to navigate resection.

2.4.3. Cy7-MO-Guided Surgery. Mice injected with Cy7-MO probe underwent the guided surgery (Cy7-MO-surgery group), and a separate group of mice underwent traditional surgery (T-surgery, no fluorescence navigation group). Based on the biodistribution results, the time point of 24 h after intravenous injection of Cy7-MO probe was chosen to conduct the surgery using NIR fluorescence imaging. During the entire operation, the orthotopic breast tumor margin was clearly visualized with the imaging system, which assisted us to perform precise resection of tumors. After the first surgery, the fluorescence and bioluminescence signals were still present, so a second operation was performed until no bioluminescence signal could be observed throughout the entire body of the mouse (Figure 4A), indicating that the breast cancer tumors were completely removed.

https://doi.org/10.1021/acsomega.3c00601
ACS Omega 2023, 8, 12481−12488

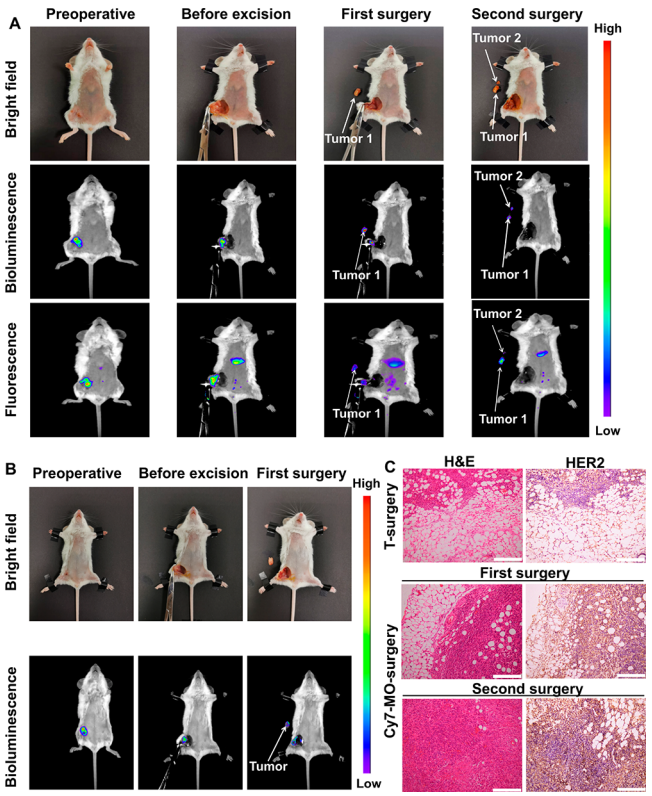

Figure 4. Surgical resection of orthotopic breast tumors. (A) Detection and resection of orthotopic breast tumors using Cy7-MO-guided surgery. (B) Resection of orthotopic breast tumors with traditional surgery (without Cy7-MO guided). (C) H&E and IHC evaluation of surgically removed tumors in the traditional and Cy7-MO guided surgery groups (scale bar = 200 μm).

However, for mice that underwent traditional surgery without Cy7-MO, orthotopic breast tumors were dissected on the basis of experience and perception. Bioluminescence evaluation was carried out to determine whether the tumor was precisely resected, as shown in Figure 4B. After the surgery, positive tumor tissue was still observed at the orthotopic breast tumor margin areas. As a result, Cy7-MO-guided surgery could achieve increased precision of surgery compared to traditional surgery by the same operator.

2.4.4. Pathological Evaluations. Human epidermal growth factor receptor 2 (HER2) is an orphan tyrosine kinase receptor belonging to the Human Epidermal Receptor family, which is a well-known negative prognostic factor in breast cancer.[34] The 4T1 cells, as a type of breast cancer cells, are highly expressed with HER2. So, imaging of the breast cancer cell surface receptor HER2 could provide additional evidence of breast tumor detection,[35] and we can determine whether the surgically removed tumor tissue is based on the H&E staining and immunohistochemical (IHC) staining for HER2.

In order to confirm the precise surgery of the tumors, the tumor tissues were subjected to H&E and IHC staining for HER2, which are shown in Figure 4C. Compared to Cy7-MO-guided surgery group, there are still tumor tissues on the site of operation in "T-surgery" group. For Cy7-MO-guided surgery group, the correct tumor tissues were completely removed in both the first and second surgery, and a negative margin was achieved. Moreover, traditional surgery dissected more normal tissue than Cy7-MO-guided surgery.

CONCLUSIONS

In summary, we designed a fluorescent probe Cy7-MO based on the heptamethine cyanine core, in which the quaternary ammonium groups were modified on each side, and a morpholine moiety was introduced on the meso-chlorine atom. The lysosomal targeting ability was verified by confocal laser scanning microscopy (CLSM) and indicated the strong affinity of morpholine group to lysosomes in Cy7-MO. Importantly, the Cy7-MO probe was well tolerable and has excellent biocompatibility. Moreover, the orthotopic breast tumor margin was clearly visualized with Cy7-MO guided and assisted us to perform precise resection of tumors, which achieved increased precision of surgery. Finally, the correct tumor tissues were completely removed, and a negative margin was achieved.

Although the Cy7-MO probe was well targeted to tumor lysosomes and delineated tumor margins so well as to guide tumor resection, it took up to 24 h to operate after injection. Moreover, it was also distributed in other tissues, such as the liver. Therefore, in subsequent studies, the probe will be loaded in nanocarriers to reduce the distribution and accumulation of the probe in other tissues and shorten the time interval between injection and surgical excision. The above work may be beneficial for clinical application, and we hope to develop a NIR Cy7-MO nanoparticle system that can be used in clinical tumor surgical navigation in the future.

EXPERIMENTAL SECTION

4.1. Materials. All the solvents used in the reactions are commercially available superdry solvents (Energy Chemical). The silica gel with a mesh of 200−300 was obtained from Shanghai Titan Scientific General-Reagent (Shanghai, China). The eluents were also produced by General-Reagent. The ^{1}H NMR and ^{13}C NMR spectra were recorded at room temperature using an Agilent 400 DD2 spectrometer (California, USA). The HRMS was measured using Thermo Scientific Q Exactive Orbitrap Mass Spectrometers (Massachusetts, USA). All other chemicals were analytical grade.

Fetal bovine serum (FBS) was purchased from AusGeneX (Molendinar, Australia), RPMI 1640 medium (with penicillin and streptomycin) was obtained from KeyGEN BioTECH (NanJing, China), trypsin EDTA (0.25%) was purchased from Gibco Invitrogen (Grand Island, USA), and cellular-grade DMSO was from Beijing Solarbio Science & Technology Co., Ltd. (Beijing, China).

4.2. Synthesis, Characterization, and Photophysical Properties of Cy7-MO. The compound 3 was prepared following the previous literature[27] without modification. The compound 3 (300 mg, 0.34 mmol), 4-(2-aminoethyl) morpholine (88.40 mg, 0.68 mmol), and triethylamine (94.5 μL, 0.68 mmol) were added to the DMF (5 mL), then the mixture was stirred at 80 °C for 4 h under nitrogen atmosphere. The solvent was removed under vacuum. The residue was purified using aluminum oxide chromatography (DCM: MeOH = 50:1) to give blue solid, yield 52%. ^{1}H NMR (400 MHz, CD_3OD) δ 7.87 (d, J = 12.7 Hz, 2H), 7.50 (d, J = 7.4 Hz, 2H), 7.44 (t, J = 7.7, 7.7 Hz, 2H), 7.31 (d, J = 7.9 Hz, 2H), 7.21 (t, J = 7.5, 7.5 Hz, 2H), 6.02 (d, J = 12.8 Hz, 2H), 4.20 (t, J = 7.4, 7.4 Hz, 4H), 4.03 (t, J = 5.7, 5.7 Hz, 2H), 3.85 (t, J = 4.5, 4.5 Hz, 4H), 3.27 (s, 18H), 2.85 (m, 4H), 2.39 (q, J = 8.7, 8.1, 8.1 Hz, 4H), 2.08 (m, 4H), 1.96 (q, J = 6.5, 6.5, 6.4 Hz, 2H), 1.81 (s, 12H). ^{13}C NMR (101 MHz, CD_3OD) δ

https://doi.org/10.1021/acsomega.3c00601
ACS Omega 2023, 8, 12481−12488

169.9, 166.6, 142.8, 139.6, 137.4, 128.2, 122.6, 121.8, 121.2, 108.6, 94.3, 66.4, 59.8, 53.4, 52.3, 45.3, 37.1, 28.0, 25.7, 25.3, 22.7, 21.4, 20.3. HRMS (ESI, $[M]^+ m/z$): Calcd for $C_{46}H_{69}N_6O$ 249.8610; Found m/z 249.8604.

4.3. Measurement of Fluorescence Quantum Yield. The fluorescence quantum yield of Cy7-MO was calculated using the following equation:

$$\phi_{FL}^{Sp} = \phi_{FL}^{St} \frac{I^{Sp}}{I^{St}} \frac{1 - 10^{-A^{St}}}{1 - 10^{-A^{Sp}}} \frac{n_{Sp}^2}{n_{Sp}^2} \quad (1)$$

where Φ was fluorescence quantum yield, I was the integrated fluorescence intensity, n was the refractive index, and A was the absorbance at the excitation wavelength. The superscript "St" and "Sp" were represented to the standard and sample, respectively. In this study, the methylene blue was used as a standard (2% in water).[36]

4.4. In Vitro Colocalization. *4.4.1. Cell Culture.* Mouse breast cancer 4T1-Luc1 cells were obtained from Zhejiang Meisen Cell Technology Co., Ltd. The cells were maintained in complete medium, which consisted of 90% basal medium (RPMI 1640, with streptomycin and penicillin) and 10% fetal bovine serum, and placed in a humidified incubator at 37 °C under 5% CO_2 atmosphere.

4.4.2. Cytotoxicity. The cytotoxicity of Cy7-MO solution against 4T1-Luc1 cells was evaluated using CCK-8 assay. The cells were seeded into a 96-well plate at a density of 7×10^3 cells per well and incubated for 24 h. Then, the medium containing Cy7-MO with different concentrations of Cy7-MO (1, 2.5, 5, 10, 50, 100, 150, 300 μM) was added to each well and incubated for a further 24 h. After the incubation for 24 h, the medium containing the Cy7-MO was aspirated and washed with 100 μL PBS. Then, 100 μL 10% CCK-8 was added to each well and incubated for a further 2 h. Finally, the plates were subjected to microplate reading (WD-2102B automatic microplate reader was purchased from Beijing Liuyi Biotechnology Co., Ltd.) for cell viability assays at a wavelength of 450 nm. Cell viability was calculated as

$$\text{cell viability } (\%) = \frac{A_s - A_b}{A_c - A_b} \times 100 \quad (2)$$

where A_s, A_c and A_b refer to the absorbance of the experimental wells, the control wells, and the blank wells, respectively.

4.4.3. Cellular Colocalization. The colocalization experiment was carried out using commercial dyes: Lyso-Tracker Green and rhodamine 123. 4T1-Luc1 cells were seeded into confocal dishes and incubated 48 h. Then, the cells were coincubated with the probe Cy7-MO (10 μM) for 30 min and Lyso-Tracker Green (10 nM) for 15 min. To further explore the colocalization ability of the probe with other organelles such as mitochondria, 4T1-Luc1 cells were coincubated with the Cy7-MO (10 μM) for 30 min and rhodamine 123 (10 nM) for 15 min. The 4T1-Luc1 cells were washed three times with PBS and kept the cells in serum-free RPMI 1640 for imaging with a CLSM (Olympus, FV3000, Japan) immediately. The images were obtained under a 488 nm excitation and 500−550 nm collection for the green channel, and a 640 nm excitation and 700−800 nm collection for the red channel. Colocalization analysis was performed by ImageJ software.

4.5. Safety Evaluation of Cy7-MO. In order to evaluate the possible toxicity arise from Cy7-MO *in vivo*, the toxicity study of Cy7-MO was conducted on normal BALB/c mice. Twelve healthy BALB/c mice were randomly assigned to two groups (n = 6 per group). On day 0, mice in one group were intravenously injected with 100 μL of Cy7-MO (0.25 mM in PBS), and mice in another group were treated with PBS for control. All mice were sacrificed at the end of the study on day 7, and their blood was collected which the serum was separated to measure biochemical indices: AST, ALT, CREA, and UREA, to assess liver and kidney function. The heart, liver, spleen, lung, and kidney of all the mice were taken, and H&E staining was conducted under standard methods to evaluate the safety of Cy7-MO on BALB/c mice.

4.6. Cy7-MO-Guided Surgical Resection. *4.6.1. Animals and Orthotopic Breast Cancer Mouse Model.* Healthy female BALB/c mice, 5−7 weeks, weight 18 ± 2 g, were purchased from SPF (Beijing) Biotechnology Co., Ltd. (Beijing, China) and housed in the animal compartment with a temperature of 25 ± 2 °C and a relative humidity of 50 ± 2%. After a week acclimation period, the animals were used for the experiments. All experimental procedure and animals care were performed in accordance with the guidelines established by the Guizhou Provincial Science Committee, and the entire project protocol was approved by the Animal Ethics Committee of Zunyi Medical University (Lunshen (2020)2-107).

The mouse mammary carcinoma 4T1-Luc1 cells (4T1-Luc1, luciferase) were taken from the exponential growth phase and resuspended in RPMI 1640, centrifuged, and washed 3 times to remove the serum. The cell concentration was adjusted to 2×10^7 cells/mL with RPMI 1640, and cell suspensions (0.1 mL/mouse) were orthotopically transplanted into the lower right mammary fat pads of the mice. The tumor volume was determined every day using a vernier caliper, and their weights were measured by an electronic scale. When the tumor volume grew up to about 100 mm^3 (tumor volume $V = ab^2/2$; a: tumor length, b: tumor width), they were used in the navigation experiment of tumor resection.

4.6.2. Biodistribution of Cy7-MO in Mice. In order to evaluate the feasibility of breast tumor detection and the biodistribution time, we randomly chose three mice bearing 4T1-luc1 tumor cells for about 5 days. The tumor bearing mice were anesthetized intramuscularly (0.05 mL/mouse) using Zoletil 50 combined with serazine hydrochloride (25 mg/kg for Zoletil 50 and 7.5 mg/kg for serazine hydrochloride), and then Cy7-MO probes (100 μL, 0.5 mM) were intravenously injected into the tumor-bearing mice using a microsyringe. Before and after injection, mice were placed in the NightOWL II LB983 small animal *in vivo* imaging system (Berthold Technologies GmbH & Co. KG) for continuous monitoring at different time points. For fluorescence imaging, it was performed with excitation at 642 nm and emission at 740 nm.

4.6.3. Validation of Tumor Location. To verify whether the tumor location marked by Cy7-MO probe was correct, and to provide comprehensive information about the tumor, 96 h after injection of Cy7-MO, 100 μL of Luc1 substrate (DTZ solution, CTCC-Luc-001, Zhejiang Meisen Cell Technology Co., Ltd.) was intraperitoneally injected, and then bioluminescence imaging and fluorescence imaging were performed successively.

4.6.4. Cy7-MO-Guided Surgery. A total of 12 mice were randomly divided into two groups: traditional surgery (T-surgery, no fluorescence navigation) and Cy7-MO fluorescence navigation surgery (Cy7-MO-surgery) groups. With the experience of a surgeon, the tumor tissues were aseptically prepped, and sterile instruments were employed to excise the tumors. For "T-surgery" group, Luc1 substrate was injected

https://doi.org/10.1021/acsomega.3c00601
ACS Omega 2023, 8, 12481−12488

intraperitoneally, and bioluminescence was observed before and after surgical resection. To locate and precisely remove the tumor, the mice in the "Cy7-MO-surgery" group were anesthetized 24 h after injection for optical imaging and tumor resection. The operative incision sites were followed by fluorescence imaging to detect if there were residual tumors left behind. When demonstrating the existence of residual tumors after the first surgery, the second surgery was performed to remove the tumors until there were no fluorescence signals. In this process, a bioluminescence signal was used to verify the accuracy of fluorescence signal. The process of Cy7-MO-guided tumor resection surgery can be seen from Figure S7.

4.6.5. Pathological Evaluations. In order to confirm the precise surgery of the tumors, the tumor tissues were soaked in 4% paraformaldehyde and subjected to H&E and IHC staining for HER2. Specifically, the tumor tissue embedding was done in paraffin, and then, tissue sections of 4 μm thickness were prepared. Finally, they were conducted for H&E staining under standard methods. Later, all the slides were observed under a microscope (Microscope: Olympus BX43, Tokyo, Japan, Multiplier: 20×).

To detect the expressions of HER2 by IHC, the tumor sections were incubated with primary rabbit monoclonal antibody against HER2 (1:100, AG1859, Beyotime Biotechnology, Shanghai, China) overnight at 4 °C followed by incubation with a secondary biotin-labeled goat antirabbit antibody (PV-9001, ZSJQ-BIO, Beijing, China) at 37 °C for 30 min. Finally, the sections were stained with DAB chromogen (ZLI-9018, ZSJQ-BIO, Beijing, China), and the cell nucleus was stained with hematoxylin for 5 min. Later, all the slides were observed under a microscope (Olympus BX43, Tokyo, Japan, and Multiplier: 20×).

4.7. Statistical Analysis. All numerical parameters were expressed as means ± standard deviation. Differences between two groups were evaluated using a Student's *t* test. Differences among experimental groups were assessed using the one-way analysis of variance (ANOVA). The *p*-value <0.05 was taken as statistically significant.

■ ASSOCIATED CONTENT

Supporting Information

The Supporting Information is available free of charge at https://pubs.acs.org/doi/10.1021/acsomega.3c00601.

Additional spectra (^{1}H NMR, ^{13}C NMR, ESI-Mass), cytotoxicity, safety evaluation, and the process of tumor resection surgery in support formation (PDF)

■ AUTHOR INFORMATION

Corresponding Authors

Jie Gao − *Key Laboratory of Basic Pharmacology of Ministry of Education and Joint International Research Laboratory of Ethnomedicine of Ministry of Education, Key Laboratory of Biocatalysis & Chiral Drug Synthesis of Guizhou Province, School of Pharmacy, and Guizhou International Scientific and Technological Cooperation Base for Medical Photo-Theranostics Technology and Innovative Drug Development, Zunyi Medical University, Zunyi, Guizhou Province 563000, China*; Email: jiegao@mail.nankai.edu.cn

Zeli Yuan − *Key Laboratory of Basic Pharmacology of Ministry of Education and Joint International Research Laboratory of Ethnomedicine of Ministry of Education, Key Laboratory of Biocatalysis & Chiral Drug Synthesis of Guizhou Province, School of Pharmacy, and Guizhou International Scientific and Technological Cooperation Base for Medical Photo-Theranostics Technology and Innovative Drug Development, Zunyi Medical University, Zunyi, Guizhou Province 563000, China*; orcid.org/0000-0001-5354-769X; Email: zlyuan@zmu.edu.cn

Authors

Yumei Wu − *Key Laboratory of Basic Pharmacology of Ministry of Education and Joint International Research Laboratory of Ethnomedicine of Ministry of Education, Key Laboratory of Biocatalysis & Chiral Drug Synthesis of Guizhou Province, School of Pharmacy, and Guizhou International Scientific and Technological Cooperation Base for Medical Photo-Theranostics Technology and Innovative Drug Development, Zunyi Medical University, Zunyi, Guizhou Province 563000, China*

Zhengjun Chen − *Key Laboratory of Basic Pharmacology of Ministry of Education and Joint International Research Laboratory of Ethnomedicine of Ministry of Education, Key Laboratory of Biocatalysis & Chiral Drug Synthesis of Guizhou Province, School of Pharmacy, and Guizhou International Scientific and Technological Cooperation Base for Medical Photo-Theranostics Technology and Innovative Drug Development, Zunyi Medical University, Zunyi, Guizhou Province 563000, China*

Dan Shen − *Key Laboratory of Basic Pharmacology of Ministry of Education and Joint International Research Laboratory of Ethnomedicine of Ministry of Education, Key Laboratory of Biocatalysis & Chiral Drug Synthesis of Guizhou Province, School of Pharmacy, and Guizhou International Scientific and Technological Cooperation Base for Medical Photo-Theranostics Technology and Innovative Drug Development, Zunyi Medical University, Zunyi, Guizhou Province 563000, China*

Zhiquan He − *Morphological Laboratory, Zunyi Medical University, Zunyi, Guizhou Province 563000, China*

Jiajia Lv − *Key Laboratory of Basic Pharmacology of Ministry of Education and Joint International Research Laboratory of Ethnomedicine of Ministry of Education, Key Laboratory of Biocatalysis & Chiral Drug Synthesis of Guizhou Province, School of Pharmacy, and Guizhou International Scientific and Technological Cooperation Base for Medical Photo-Theranostics Technology and Innovative Drug Development, Zunyi Medical University, Zunyi, Guizhou Province 563000, China*

Hongyu Li − *Key Laboratory of Basic Pharmacology of Ministry of Education and Joint International Research Laboratory of Ethnomedicine of Ministry of Education, Key Laboratory of Biocatalysis & Chiral Drug Synthesis of Guizhou Province, School of Pharmacy, and Guizhou International Scientific and Technological Cooperation Base for Medical Photo-Theranostics Technology and Innovative Drug Development, Zunyi Medical University, Zunyi, Guizhou Province 563000, China*; orcid.org/0000-0001-7359-678X

Mingyan Yang − *Key Laboratory of Basic Pharmacology of Ministry of Education and Joint International Research Laboratory of Ethnomedicine of Ministry of Education, Key Laboratory of Biocatalysis & Chiral Drug Synthesis of Guizhou Province, School of Pharmacy, and Guizhou International Scientific and Technological Cooperation Base*

https://doi.org/10.1021/acsomega.3c00601
ACS Omega 2023, 8, 12481−12488

for Medical Photo-Theranostics Technology and Innovative Drug Development, Zunyi Medical University, Zunyi, Guizhou Province 563000, China

Jun Tan − *Department of Histology and Embryology, Zunyi Medical University, Zunyi, Guizhou Province 563000, China*

Jianrong Yuan − *Key Laboratory of Basic Pharmacology of Ministry of Education and Joint International Research Laboratory of Ethnomedicine of Ministry of Education, Key Laboratory of Biocatalysis & Chiral Drug Synthesis of Guizhou Province, School of Pharmacy, and Guizhou International Scientific and Technological Cooperation Base for Medical Photo-Theranostics Technology and Innovative Drug Development, Zunyi Medical University, Zunyi, Guizhou Province 563000, China*

Complete contact information is available at: https://pubs.acs.org/10.1021/acsomega.3c00601

Notes

The authors declare no competing financial interest.

■ ACKNOWLEDGMENTS

We are grateful for the financial support from the Natural Science Foundation of China (82060626, 81360471), Guizhou Science and Technology Support Program ([2020]4Y158), Talents of Guizhou Science and Technology Cooperation Platform ([2020]4104), Guizhou Science and Technology Plan (Qianke He Foundation-ZK [2021] General 035), the Excellent Youth Scientific Talents of Guizhou ([2021]5638), Zunyi Science and Technology Plan (Zunshikehe HZ Zi [2020]46), Platform talents of Qiankehe ([2018]5772-053), Cultivation project plan of new seedling cultivation and innovation exploration special project of Zunyi Medical University, and Platform talents of Qiankehe ([2018] 5772-030).

■ REFERENCES

(1) Lei, S.; Zheng, R.; Zhang, S.; Wang, S.; Chen, R.; Sun, K.; Zeng, H.; Zhou, J.; Wei, W. Global patterns of breast cancer incidence and mortality: A population-based cancer registry data analysis from 2000 to 2020. *Cancer Commun. (Lond)* **2021**, *41* (11), 1183−1194.

(2) Qiu, H.; Cao, S.; Xu, R. Cancer incidence, mortality, and burden in China: a time-trend analysis and comparison with the United States and United Kingdom based on the global epidemiological data released in 2020. *Cancer Commun. (Lond)* **2021**, *41* (10), 1037−1048.

(3) Sung, H.; Ferlay, J.; Siegel, R. L.; Laversanne, M.; Soerjomataram, I.; Jemal, A.; Bray, F. Global Cancer Statistics 2020: GLOBOCAN Estimates of Incidence and Mortality Worldwide for 36 Cancers in 185 Countries. *CA Cancer J. Clin* **2021**, *71* (3), 209−249.

(4) Lukianova-Hleb, E. Y.; Kim, Y.-S.; Belatsarkouski, I.; Gillenwater, A. M.; O'Neill, B. E.; Lapotko, D. O. Intraoperative diagnostics and elimination of residual microtumours with plasmonic nanobubbles. *Nat. Nanotechnol* **2016**, *11* (6), 525−532.

(5) Wang, P.; Fan, Y.; Lu, L.; Liu, L.; Fan, L.; Zhao, M.; Xie, Y.; Xu, C.; Zhang, F. NIR-II nanoprobes in-vivo assembly to improve image-guided surgery for metastatic ovarian cancer. *Nat. Commun.* **2018**, *9* (1), 2898.

(6) Lan, L.; Xia, Y.; Li, R.; Liu, K.; Mai, J.; Medley, J. A.; Obeng-Gyasi, S.; Han, L. K.; Wang, P.; Cheng, J. X. A fiber optoacoustic guide with augmented reality for precision breast-conserving surgery. *Light Sci. Appl.* **2018**, *7*, 2.

(7) Tipirneni, K. E.; Warram, J. M.; Moore, L. S.; Prince, A. C.; de Boer, E.; Jani, A. H.; Wapnir, I. L.; Liao, J. C.; Bouvet, M.; Behnke, N. K.; Hawn, M. T.; Poultsides, G. A.; Vahrmeijer, A. L.; Carroll, W. R.; Zinn, K. R.; Rosenthal, E. Oncologic Procedures Amenable to Fluorescence-guided Surgery. *Ann. Surg* **2017**, *266* (1), 36−47.

(8) Crippa, S.; Giannone, F.; Lena, M. S.; Falconi, M. ASO Author Reflections: R Status Is a Relevant Prognostic Factor for Recurrence and Survival After Pancreatic Head Resection for Ductal Adenocarcinoma. *Ann. Surg Oncol* **2021**, *28* (8), 4613−4614.

(9) Chen, J.; Liu, L.; Motevalli, S. M.; Wu, X.; Yang, X.-H.; Li, X.; Han, L.; Magrini, A.; Guo, W.; Chang, J.; Bottini, M.; Liang, X.-J. Light-Triggered Retention and Cascaded Therapy of Albumin-Based Theranostic Nanomedicines to Alleviate Tumor Adaptive Treatment Tolerance. *Adv. Funct. Mater.* **2018**, *28* (17), 1707291.

(10) Fan, Q.; Cheng, K.; Yang, Z.; Zhang, R.; Yang, M.; Hu, X.; Ma, X.; Bu, L.; Lu, X.; Xiong, X.; Huang, W.; Zhao, H.; Cheng, Z. Perylene-diimide-based nanoparticles as highly efficient photoacoustic agents for deep brain tumor imaging in living mice. *Adv. Mater.* **2015**, *27* (5), 843−7.

(11) Tummers, W. S.; Warram, J. M.; Tipirneni, K. E.; Fengler, J.; Jacobs, P.; Shankar, L.; Henderson, L.; Ballard, B.; Pfefer, T. J.; Pogue, B. W.; Weichert, J. P.; Bouvet, M.; Sorger, J.; Contag, C. H.; Frangioni, J. V.; Tweedle, M. F.; Basilion, J. P.; Gambhir, S. S.; Rosenthal, E. L. Regulatory Aspects of Optical Methods and Exogenous Targets for Cancer Detection. *Cancer Res.* **2017**, *77* (9), 2197−2206.

(12) Yang, R. Q.; Chen, M.; Zhang, Q.; Gao, Y. Y.; Lou, K. L.; Lin, T. T.; Huang, W. H.; Zeng, Y. Z.; Zhang, Y. Q.; Dang, Y. Y.; Ren, L.; Zhang, G. J. Development and Preclinical Evaluation of a Near-Infrared Fluorescence Probe Based on Tailored Hepatitis B Core Particles for Imaging-Guided Surgery in Breast Cancer. *Int. J. Nanomedicine* **2022**, *17*, 1343−1360.

(13) Qi, J.; Li, J.; Liu, R.; Li, Q.; Zhang, H.; Lam, J. W. Y.; Kwok, R. T. K.; Liu, D.; Ding, D.; Tang, B. Z. Boosting Fluorescence-Photoacoustic-Raman Properties in One Fluorophore for Precise Cancer Surgery. *Chem.* **2019**, *5* (10), 2657−2677.

(14) Zhang, L.; Liu, X. A.; Gillis, K. D.; Glass, T. E. A High-Affinity Fluorescent Sensor for Catecholamine: Application to Monitoring Norepinephrine Exocytosis. *Angew. Chem., Int. Ed. Engl.* **2019**, *58* (23), 7611−7614.

(15) Tao, J.; Tu, Y.; Liu, P.; Tang, Y.; Wang, F.; Li, Z.; Li, C.; Li, Y.; Ma, Y.; Gu, Y. Detection of colorectal cancer using a small molecular fluorescent probe targeted against c-Met. *Talanta* **2021**, *226*, 122128.

(16) Saremi, B.; Yao, T.; Yuan, B. Thermo- and pH-sensitive nanoparticles of poly (N-isopropylacrylamide-decenoic acid-1-vinylimidazole) for ultrasound switchable fluorescence imaging. *Exp Biol. Med. (Maywood)* **2022**, *247* (12), 1005−1012.

(17) Kang, H.; Kang, M. W.; Kashiwagi, S.; Choi, H. S. NIR fluorescence imaging and treatment for cancer immunotherapy. *J. Immunother Cancer* **2022**, *10* (7), e004936.

(18) Gomes, A. J.; Lunardi, L. O.; Marchetti, J. M.; Lunardi, C. N.; Tedesco, A. C. Indocyanine green nanoparticles useful for photomedicine. *Photomed Laser Surg* **2006**, *24* (4), 514−521.

(19) Egloff-Juras, C.; Bezdetnaya, L.; Dolivet, G.; Lassalle, H. P. NIR fluorescence-guided tumor surgery: new strategies for the use of indocyanine green. *Int. J. Nanomedicine* **2019**, *14*, 7823−7838.

(20) Dai, Y.; Tang, Y.; Huang, W.; Zhao, Y.; Gao, X.; Gu, Y. Multimodal imaging probe for EpCAM overexpressed in breast cancer. *Talanta* **2022**, *250*, 123715.

(21) Zhu, Y. X.; Jia, H. R.; Gao, G.; Pan, G. Y.; Jiang, Y. W.; Li, P.; Zhou, N.; Li, C.; She, C.; Ulrich, N. W.; Chen, Z.; Wu, F. G. Mitochondria-acting nanomicelles for destruction of cancer cells via excessive mitophagy/autophagy-driven lethal energy depletion and phototherapy. *Biomaterials* **2020**, *232*, 119668.

(22) Gao, G.; Jiang, Y. W.; Sun, W.; Guo, Y.; Jia, H. R.; Yu, X. W.; Pan, G. Y.; Wu, F. G. Molecular Targeting-Mediated Mild-Temperature Photothermal Therapy with a Smart Albumin-Based Nanodrug. *Small* **2019**, *15* (33), 1900501.

(23) Pan, G. Y.; Jia, H. R.; Zhu, Y. X.; Wang, R. H.; Wu, F. G.; Chen, Z. Dual Channel Activatable Cyanine Dye for Mitochondrial Imaging and Mitochondria-Targeted Cancer Theranostics. *ACS biomaterials science & engineering* **2017**, *3* (12), 3596−3606.

(24) Alachouzos, G.; Schulte, A. M.; Mondal, A.; Szymanski, W.; Feringa, B. L. Computational Design, Synthesis, and Photochemistry of Cy7-PPG, an Efficient NIR-Activated Photolabile Protecting Group for Therapeutic Applications. *Angew. Chem., Int. Ed. Engl.* **2022**, *61* (27), e202201308.
(25) Jiang, Z.; Pflug, K.; Usama, S. M.; Kuai, D.; Yan, X.; Sitcheran, R.; Burgess, K. Cyanine-Gemcitabine Conjugates as Targeted Theranostic Agents for Glioblastoma Tumor Cells. *J. Med. Chem.* **2019**, *62* (20), 9236−9245.
(26) Zhang, L.; Jia, H.; Liu, X.; Zou, Y.; Sun, J.; Liu, M.; Jia, S.; Liu, N.; Li, Y.; Wang, Q. Heptamethine Cyanine-Based Application for Cancer Theranostics. *Front Pharmacol* **2022**, *12*, 764654.
(27) Choi, H. S.; Nasr, K.; Alyabyev, S.; Feith, D.; Lee, J. H.; Kim, S. H.; Ashitate, Y.; Hyun, H.; Patonay, G.; Strekowski, L.; Henary, M.; Frangioni, J. V. Synthesis and in vivo fate of zwitterionic near-infrared fluorophores. *Angew. Chem., Int. Ed. Engl.* **2011**, *50* (28), 6258−63.
(28) Ramu, V.; Gautam, S.; Kondaiah, P.; Chakravarty, A. R. Diplatinum(II) Catecholate of Photoactive Boron-Dipyrromethene for Lysosome-Targeted Photodynamic Therapy in Red Light. *Inorg. Chem.* **2019**, *58* (14), 9067−9075.
(29) Mai, Y.; Qu, X.; Ding, S.; Lv, J.; Li, X.; Gao, P.; Liu, Y.; Yuan, Z. Improved IR780 derivatives bearing morpholine group as tumor-targeted therapeutic agent for near-infrared fluorescence imaging and photodynamic therapy. *Dyes Pigm.* **2020**, *177*, 107979.
(30) Mindell, J. A. Lysosomal Acidification Mechanisms. *Annu. Rev. Physiol.* **2012**, *74*, 69−86.
(31) Chen, X.; Zhang, X.; Xia, L. Y.; Wang, H. Y.; Chen, Z.; Wu, F. G. One-Step Synthesis of Ultrasmall and Ultrabright Organosilica Nanodots with 100% Photoluminescence Quantum Yield: Long-Term Lysosome Imaging in Living, Fixed, and Permeabilized Cells. *Nano Lett.* **2018**, *18* (2), 1159−1167.
(32) Chen, X.; Zhang, X.; Wu, F.-G. Ultrasmall green-emitting carbon nanodots with 80% photoluminescence quantum yield for lysosome imaging. *Chin. Chem. Lett.* **2021**, *32* (10), 3048−3052.
(33) Zhang, X.; Zhan, C.; Xiao, Y.; Tang, X. Measurement and comparisons of organ weight, organ coefficient, hematological parameters and hematological biochemical parameters of specific pathogen free Balbc mice. *Journal of Clinical Rehabilitative Tissue Engineering Research* **2011**, *15* (41), 7734−7737.
(34) Marchio, C.; Annaratone, L.; Marques, A.; Casorzo, L.; Berrino, E.; Sapino, A. Evolving concepts in HER2 evaluation in breast cancer: Heterogeneity, HER2-low carcinomas and beyond. *Semin Cancer Biol.* **2021**, *72*, 123−135.
(35) Chi, C.; Zhang, Q.; Mao, Y.; Kou, D.; Qiu, J.; Ye, J.; Wang, J.; Wang, Z.; Du, Y.; Tian, J. Increased precision of orthotopic and metastatic breast cancer surgery guided by matrix metalloproteinase-activatable near-infrared fluorescence probes. *Sci. Rep* **2015**, *5*, 14197.
(36) Chin, P. T.; Welling, M. M.; Meskers, S. C.; Valdes Olmos, R. A.; Tanke, H.; van Leeuwen, F. W. Optical imaging as an expansion of nuclear medicine: Cerenkov-based luminescence vs fluorescence-based luminescence. *Eur. J. Nucl. Med. Mol. Imaging* **2013**, *40* (8), 1283−91.

https://doi.org/10.1021/acsomega.3c00601
ACS Omega 2023, 8, 12481−12488